

EFFECT OF UNCERTAINTY IN CALIBRATION ON THE CORRELATION STRUCTURE OF THE RHEUMATOID FACTOR IMMUNOASSAY CALIBRATION FUNCTION

Varun Ramamohan

Research Triangle Institute - Health Solutions
300 Park Offices Drive
Durham, NC 27703, USA

James T. Abbott

Roche Diagnostics Corporation
9115 Hague Road,
PO Box 50457
Indianapolis, IN 46250-0457, USA

Yuehwern Yih

School of Industrial Engineering
Purdue University
West Lafayette, IN 47907, USA

ABSTRACT

Clinical laboratory measurements are vital to the medical decision-making process, and specifically, measurement of rheumatoid factor antibodies is part of the disease criteria for various autoimmune conditions. Uncertainty estimates describe the quality of the measurement process, and uncertainty in calibration of the instrument used in the measurement can be an important contributor to the net measurement uncertainty. In this paper, we develop a physics-based mathematical model of the rheumatoid factor measurement process, or assay, and then use the Monte Carlo method to investigate the effect of uncertainty in the calibration process on the correlation structure of the parameters of the calibration function. We demonstrate numerically that a change in uncertainty of the calibration process can be quantified by one of two metrics: (1) the 1-norm condition number of the correlation matrix, or (2) the sum of the absolute values of the correlation coefficients between the parameters of the calibration function.

1 INTRODUCTION

The need for providing estimates of uncertainty for clinical laboratory measurement results has been recognized by the United States Congress by its passage of the Clinical Laboratory Improvement Amendments (CLIA) Act in 1988, which mandates recording estimates of measurement uncertainty and establishing validated quality control (QC) processes in the clinical laboratory. A robust calibration process is a critical part of establishing a valid QC process, and uncertainty in the calibration process can be a significant contributor to the inaccuracy and imprecision of the result of a measurement. In this study, we develop a physics-based Monte Carlo simulation model that estimates the uncertainty associated with the measurement of the rheumatoid factor (RF) group of antibodies in the clinical laboratory. This simulation model is then used to investigate the effect of uncertainty in the calibration process on the correlation structure of the parameters of the calibration function and identify metrics that quantify change in the uncertainty of the calibration process of the RF assay without requiring the use of a benchmark measurement.

Measurement uncertainty is defined in the ISO-BIPM-OIML-IUPAC Guide to the Expression of Uncertainty in Measurement (GUM) (BIPM et al. 1993, JCGM-100 2008) as “any parameter that characterizes

the dispersion of the distribution of the values that can be attributed to the result of a measurement". In this work, we use the standard deviation as the measure of uncertainty since the distributions of the sources of uncertainty within the measurement process are all characterized to be Gaussian, and the distribution of the measurement result, or the measurand, is also found to be Gaussian.

A clinical laboratory measurement process, widely referred to as a clinical *assay*, consists of three stages. The first, the preanalytical stage, comprises all activities performed prior to patient sample analysis (Burtis et al. 2012). The second, the analytical stage, involves instrument calibration and subsequent analysis of the patient sample on the calibrated instrument. The final post-analytical stage consists of recording, reporting and interpreting the measurement. In this study, we model only the analytical stage, since identifying and modeling the variation of the numerous sources of uncertainty associated with the preanalytical stage merits a separate study in itself. Uncertainty in the postanalytical stage is typically introduced due to human error in recording or reporting of the measurement result, and hence does not lie within the scope of this study.

RF consists of a group of slightly different medically significant antibodies, and high levels in the blood of these antibodies are commonly associated with various autoimmune diseases (Ferri 2012). Since RF is not a single antibody, and consists of a group of antibodies, their units of measure are International Units per milliliter, IU/mL, and not mass units such as milligrams per deciliter. They will henceforth collectively be referred to as "antibody" to maintain economy in terminology.

The RF assay is performed on the Roche Diagnostics P-Modular Analytics measurement system. One of the reactants (the antigen) for the assay chemical reaction is supplied by the reagents. The RF required for the assay is supplied by the patient sample or a calibrator. The bioanalytical principle underpinning the measurement process is immunoturbidimetry. The chemical reaction occurs between the antigen and the antibody (RF), wherein the antigen and the antibody bind to form the antigen-antibody complex. This antigen-antibody complex is insoluble in the reaction mixture, and hence is a visible product of the reaction, known as the *precipitate*. The process of formation of the insoluble antigen-antibody complex is known as *agglutination* and it increases the turbidity of the reaction mixture. The optical absorbance recorded as part of the RF assay is directly proportional to the concentration of the antigen-antibody complex at that point in time, and hence is a measure of turbidity of the reaction mixture. The measured optical absorbance is converted into RF concentration by a nonlinear calibration function.

Several studies have previously attempted to estimate the uncertainty associated with specific clinical laboratory measurement processes, and a few prominent studies are listed here (Kallner 1999, Borg et al. 2002, Suchanek and Robouch 2009, Rami and Canalias 2014). These studies use one of the following two methods: (1) application of the analytical rules for the estimation of measurement uncertainty provided in the GUM to combine the uncertainties of individual components of the measurement process; or (2) top-down estimation of assay measurement uncertainty; that is, the uncertainty is estimated from experimental data for the measurement result, represented by a parameter such as the standard deviation.

We identified very few studies that model the uncertainty associated with the turbidimetric determination of immunoprotein concentration levels. We identified two studies that involved the analytical modeling and estimation of the measurement uncertainty of immunoassays (Borg et al. 2002, Suchanek and Robouch 2009). Borg and colleagues in 2002 applied the systematic approach for modeling the uncertainty of analytical chemistry measurements described by Kristiansen in 2001 (Kristiansen 2001) to establish uncertainty budgets for four sandwich enzyme-linked immunosorbent assays (ELISAs): interleukin-4, interleukin-5, interferon- γ and tumor necrosis factor- α . This approach involves identifying and characterizing the sources of uncertainty operating within the measurement process, and then applying the law of propagation of uncertainty to estimate the assay uncertainty.

Suchanek and Robouch in 2009 (Suchanek and Robouch 2009) developed a model of measurement uncertainty of the *toxoplasma gondii* antibody ELISA test kit. Their model was based on a nonlinear relationship between analyte concentration and measured optical absorbance; however, the authors used a linear bracketing method to convert the measured optical absorbance into the desired analyte concentration.

The authors used the Kragten spreadsheet automation of the law of propagation of uncertainty to estimate the net assay uncertainty (Kragten 1994).

Both studies discussed above develop models that apply multiplicative factors that describe the uncertainty of the sources of variation to the measured quantities, and then utilize the law of propagation of uncertainty to estimate the combined measurement uncertainty of the assay. In this study, we apply a systems engineering perspective to develop a physics-based mathematical model of the measurement process, and then use the Monte Carlo method to estimate the net measurement uncertainty. The use of a systems engineering approach to model clinical assays and estimate their associated uncertainty was first suggested by Aronsson et al. in 1974 (Aronsson, de Verdier, and Groth 1974), and later by Krouwer (Krouwer 2002).

In this work, we apply a similar systems engineering perspective to model measurement uncertainty. This involves developing a mathematical model of the RF immunoassay that describes its biochemistry as well as the operational aspects of the measurement process (calibration protocols, patient sample analysis protocols, etc.). The Monte Carlo method is then used to estimate the uncertainty associated with model, and also to quantify the contributions of each measurement system of the measurement system to the net measurement uncertainty. The use of the Monte Carlo method to estimate measurement uncertainty is indicated if at least one of the following conditions are applicable to the model of the measurement process: a.) the measurement system model is required to be non-linear; b.) estimation of the degrees of freedom of the sources of uncertainty operating within the measurement system is not possible, which is the case when their variation is characterized by a non-statistical ad-hoc method; and c.) the distribution of the measurement result or any of the sources of uncertainty is not Gaussian (JCGM-101 2008). The first two conditions apply in the case of our model. The Monte Carlo method enables conducting simulation experiments with the model, and therefore facilitates extraction of information about the measurement system that would otherwise require performing laboratory experiments. This is demonstrated by using the simulation model to quantify the effect of uncertainty in the calibration process on the correlation matrix associated with the parameters of the calibration function, and consequently the use of the 1-norm condition number and the sum of the absolute values of the correlation coefficients between the calibration parameters as metrics that quantify the change in uncertainty in the calibration process.

This study was carried out jointly with the Roche Diagnostics Corporation in Indianapolis, IN (USA).

2 MODEL DEVELOPMENT

For the RF assay, the quantity to be measured or the measurand is the concentration of RF antibodies in the patient sample. The RF assay is an immunoassay, and the physical principle underlying its measurement is immunoturbidimetry, which involves the determination of the turbidity of the reaction mixture. The turbidity of the reaction mixture increases due to the increase in concentration of the insoluble antigen-antibody complex that is formed as a result of the binding that occurs between the antibody and the antigen. This binding process is expressed as a chemical reaction below:



Here Ag and Ab represent the antibody (RF antibodies) and antigen (latex-particle coated human antigens) respectively, and $AgAb$ is the antigen-antibody complex. The terms k_1 and k_{-1} are the rate constants of the forward and backward reactions, respectively. Two reagents, R_1 and R_2 , and the patient sample S are pipetted into the reaction cell where the binding occurs. R_1 provided the metal ion buffer and the preservatives necessary for the chemical reaction, and R_2 supplies the antigen that binds to the RF antibodies in the patient sample. Two optical absorbance measurements are recorded during the assay analysis process. The first measurement, denoted by $A_{x(0)}$, is made at time $t = 0$ prior to the addition of R_2 to the reaction mixture, and the second measurement, denoted by A_x is made 5.4 minutes after the first measurement is made. Since the first measurement is made at $t = 0$ before R_2 is added, the absorbance of

the reaction mixture at that point can be considered to be zero for all practical purposes. This assumption was made after consulting with the instrument manufacturer.

The volumes of the reagents are represented by V_{r1} and V_{r2} . The volume of the calibrator or patient sample is denoted by V_s .

The difference between optical absorbance measurements A_x and A_0 is converted into the RF concentration in the patient sample, denoted by C_x , by a nonlinear calibration function given below. Since we assume $A_{x(0)}$ to be zero, only the term A_x appears hereafter, and in the expression below.

$$C_x = \left[\frac{(a - (A_x - B))}{b (A_x - B)} \right]^{1/c} \quad (2)$$

This is the inverse log-logit function. Here, a , b , c and B are the parameters of the calibration function. Equation 2 has four parameters of unknown value, and therefore a minimum of four calibrators are required to characterize the calibration function. We refer to these calibrators as Ab_1 , Ab_2 , Ab_3 , and Ab_4 .

The analytical stage of the assay analysis process can be considered as consisting of two phases: the calibration phase, wherein the instrument is calibrated using standard solutions (solutions with known RF concentrations) and the values of the calibration function parameters are estimated; and the sample analysis phase, wherein the sample with unknown RF concentration is analyzed by the calibrated instrument. We now describe the development of the calibration phase component of the model.

2.1 Calibration Phase

The values of the calibration parameters a , b , c , and B are estimated in this phase. These parameters are estimated by using four calibrators - solutions with known RF concentration - and measuring their corresponding optical absorbance values. These four known RF concentration and their optical absorbance measurements are used to solve for the values of the four calibration parameters. Prior to describing how we model the uncertainty in the calibration process, we must mention the use of a reference function to generate absorbance values corresponding to different RF concentrations for the purposes of the simulation. This reference function is established using QC data provided by the manufacturer, and its parameters are assumed to be error-free. The values of absorbance (corresponding to known RF concentration) generated by this reference function are also therefore treated as ‘true/reference’ values.

We now describe the process by which uncertainty is introduced into a single calibrator measurement. Let $[Ab]$ represent the desired RF concentration in a calibrator sample. Three sources of calibrator uncertainty were identified to be associated the calibrator: calibrator set-point uncertainty (u_{c1}), vial to vial variability (u_{c2}) and calibrator reconstituted stability ($u_{c3(t)}$). Calibrator set-point uncertainty is the uncertainty in the RF concentration of the calibrator introduced during manufacturing and prior to its use in the laboratory. Vial-to-vial variability refers to the uncertainty introduced in the RF concentration while preparing different vials of the calibrator supplied by the manufacturer. Finally, calibrator reconstituted stability quantifies the deterioration (percentage decrease in RF concentration per day) of the sample when the calibrator vial is stored and reconstituted after use each day, for up to, say, N days.

When these are introduced into the model, the value of $[Ab]$ changes according to the following equation:

$$[Ab]' = [Ab] (1 + u_{c1}) (1 + u_{c2}) \prod_{t=1}^N (1 + u_{c3(t)}) \quad (3)$$

The variation of the sources of calibrator uncertainty, along with the others identified as associated with the measurement process, is characterized by fitting appropriate probability distributions to the specifications provided by the instrument manufacturer for each source of uncertainty. This method of characterizing the variation of the sources of uncertainty was used because experimental data was not available for the sources of uncertainty. As an example, specifications for calibrator set-point uncertainty were provided by the instrument manufacturer in the form of a coefficient of variation (CV) of 0.1%. After discussion with

the manufacturer, a Gaussian distribution with a mean of 0% and a standard deviation of 0.1% was assumed to quantify the variation in the calibrator RF concentration due to set-point uncertainty. The mean of the Gaussian distribution was assumed to be 0% based on the manufacturer’s judgment that systematic errors in the calibrator manufacturing process were negligible. Therefore, at a desired calibrator RF concentration of 100 IU/mL, the actual concentration would be described by a Gaussian distribution with a mean of 100 IU/mL and a standard deviation of 0.1 IU/mL.

The measured RF concentration in the calibrator is also changed by the sources of uncertainty operating within the instrument. Three key sources of uncertainty are associated with the instrument: sample pipetting uncertainty, reagent pipetting uncertainty and photometer uncertainty. Sample and reagent pipetting uncertainty describe the uncertainty in the volumes of the sample and reagents pipetted into the reaction cell, and hence yield a change in the total volume of the reaction mixture and the number of molecules of the antigen and antibody in the reaction mixture prior to the beginning of the reaction. In other words, their effect on the measurement process occurs at time $t = 0$. However, photometer uncertainty changes the absorbance measurement recorded at $t = 5.4$ minutes. The variation of these sources of uncertainty are also characterized in a manner similar to that of the sources of calibrator uncertainty, and hence are also described by Gaussian distributions. The parameters of the distributions of all the sources of uncertainty operating within the measurement process are provided in Table 1. An assumption of zero bias was made based on the manufacturer’s observation of negligible bias associated with all sources of uncertainty except reconstituted stability.

Table 1: Sources of uncertainty associated with the RF assay

| Source of uncertainty | Distribution | Mean (%) | SD (%) | Notes |
|----------------------------------|--------------|----------|--------|------------------------------------|
| Calibrator set-point uncertainty | Gaussian | 0.00 | 0.10 | Daily decrease in RF concentration |
| Vial-to-vial variability | Gaussian | 0.00 | 1.50 | |
| Reconstituted stability | Gaussian | -1.25 | 0.42 | |
| Sample pipetting uncertainty | Gaussian | 0.00 | 1.50 | |
| Reagent pipetting uncertainty | Gaussian | 0.00 | 4.00 | |
| Photometer uncertainty | Gaussian | 0.00 | 0.15 | |

We now describe the derivation of the effect of sample and reagent pipetting uncertainty on the optical absorbance measurements recorded during the assay.

We begin with the assumption that the optical absorbance at time t , denoted by A , is proportional to the concentration of the antigen-antibody complex in the reaction mixture at time t (denoted by $[AgAb]$). That is:

$$A = k [AgAb] + A_0 \tag{4}$$

Here k is the molar extinction coefficient, A_0 denotes the value of the absorbance when the $AgAb$ concentration is zero. Reaction 1 can be thought of as a first order reaction with the rate of the forward reaction dependent only on the concentration of the antibody (in IU/mL), since the antigen is present in an amount that is significantly in excess of the antibody. The rate of the reaction can also be expressed in terms of the formation of the product, as in the equation below:

$$\frac{d[AgAb]}{dt} = k_1 [Ab] \tag{5}$$

Here $[Ab]$ represents the RF concentration in IU/mL in the reaction mixture at time t . Now the rate of the reaction can also be expressed as the rate of decrease in concentration of RF. This is expressed in the equation below:

$$- \frac{d[Ab]}{dt} = k_1 [Ab] \tag{6}$$

Integrating the above rate equation results in the following:

$$-\int_{[Ab_0]}^{[Ab]} \frac{d[Ab]}{[Ab]} = -k_1 \int_0^t dt$$

$$\ln \left(\frac{[Ab]}{[Ab_0]} \right) = -k_1 t$$

Exponentiating both sides, we have:

$$[Ab] = [Ab_0] e^{-k_1 t} \quad (7)$$

Using the above expression to substitute for $[Ab]$ in Equation 5, we have:

$$\frac{d[AgAb]}{dt} = k_1 [Ab_0] e^{-k_1 t} \quad (8)$$

We integrate the above equation to obtain the relationship between the antigen-antibody complex concentration at time t , the initial amount of the antibody and time.

$$\int_{[AgAb_0]}^{[AgAb]} d[AgAb] = k_1 [Ab_0] \int_0^t e^{-k_1 t} dt$$

Evaluating the above integral yields:

$$[AgAb] = [Ab_0] (1 - e^{-k_1 t}) \quad (9)$$

Substituting the expression for $[AgAb]$ in equation 4, we obtain the relationship between optical absorbance, concentrate of antibody at time $t = 0$ and time.

$$A = k [Ab_0] (1 - e^{-k_1 t}) + A_0 \quad (10)$$

Now, at $t = 0$, the antibody concentration in the reaction mixture can be written as the ratio of the number of units of the antibody $N_{Ab(0)}$ to the volume of the reaction mixture V . That is, the above equation can be written as:

$$A = k \left(\frac{N_{Ab(0)}}{V} \right) (1 - e^{-k_1 t}) + A_0 \quad (11)$$

Further, the number of units of the antibody $N_{Ab(0)}$ can also be written as the product of the antibody concentration (in IU/mL) $[Ab_s]$ in the sample S and its volume V_s . The distinction between the terms $[Ab_0]$ and $[Ab_s]$ must be emphasized here: the former refers to the desired RF concentration in the reaction mixture at time $t = 0$, and the latter to the desired RF concentration in the patient sample S after it is pipetted out and before it is added to the reaction mixture. Therefore, the above equation can be written as:

$$A = k \left(\frac{[Ab_s] V_s}{V} \right) (1 - e^{-k_1 t}) + A_0 \quad (12)$$

The total volume of the reaction mixture V is the sum of the sample and reagent volumes V_s , V_{r1} and V_{r2} . We now introduce pipetting uncertainty into the model. We denote the fractional change in sample volume due to sample pipetting uncertainty as x , the fractional change in reagent volumes due to reagent pipetting uncertainty as y_1 and y_2 , and the fractional change in total reaction mixture volume as z . Then,

$$V_s + \delta V_s = V_s (1 + x) \quad (13a)$$

$$V_{r1} + \delta V_{r1} = V_{r1} (1 + y_1) \quad (13b)$$

$$V_{r2} + \delta V_{r2} = V_{r2} (1 + y_2) \quad (13c)$$

$$V + \delta V = V (1 + z) \quad (13d)$$

Now, using the fact that $V = V_s + V_{r1} + V_{r2}$, we have the following:

$$V + \delta V = V_s (1 + x) + V_{r1} (1 + y_1) + V_{r2} (1 + y_2) \quad (14a)$$

That is,

$$V + \delta V = V_s + V_{r1} + V_{r2} + x V_s + y_1 V_{r1} + y_2 V_{r2} \quad (14b)$$

and

$$\delta V = x V_s + y_1 V_{r1} + y_2 V_{r2} \quad (14c)$$

Uncertainty in the instrument may also occur as an error in the time at which the absorbance measurement is recorded. This will change the extent to which the reaction has occurred, and in turn the optical absorbance measured ostensibly at time t . We refer to this uncertainty in the time of measurement as *clock uncertainty*. We denote this change (error) in time of measurement as δt and the fractional change in the desired time of measurement t as u_t . If we denote the change in optical absorbance measured at time t as δA_t , then the optical absorbance after the incorporation of reagent and sample pipetting uncertainty is written as:

$$A + \delta A = k \left[\frac{[Ab_s](V_s + \delta V_s)}{V + \delta V} \right] (1 - e^{-k_1(t+\delta t)}) + A_0 \quad (15)$$

Using Equations 13a through 13d, the above expression is rewritten as:

$$A + \delta A = k [Ab_s] \frac{V_s}{V} \left[\frac{1+x}{1+z} \right] (1 - e^{-k_1(t+\delta t)}) + A_0 \quad (16)$$

Subtracting Equation 12 from Equation 16, we derive the change in optical absorbance due to pipetting uncertainty and clock uncertainty:

$$\delta A = k [Ab_s] \frac{V_s}{V} \left[\frac{(1+x)(1 - e^{-k_1(t+\delta t)})}{1+z} - (1 - e^{-k_1 t}) \right] \quad (17)$$

We denote the above fractional change in optical absorbance at time t due to pipetting and clock uncertainty, $\delta A/A$, by the term u_{pc} . Now, equation 17 denotes the change in absorbance at time t from the desired value that occurs prior to recording the absorbance measurement. When the measurement is recorded, the uncertainty due to the photometer changes the absorbance further by the fractional amount u_p . Therefore, the final expression for optical absorbance after incorporating instrument uncertainty into the model is given below:

$$A' = A (1 + u_{pc}) (1 + u_p) \quad (18)$$

The above equation denotes the value of absorbance after all sources of uncertainty affecting the optical absorbance measurement have been incorporated into the model. This process is repeated for each of the four calibrators, which yields four values of RF concentrations (in IU/mL) $[Ab_1]'$, $[Ab_2]'$, $[Ab_3]'$ and $[Ab_4]'$ and four corresponding optical absorbance measurements $[A_1]'$, $[A_2]'$, $[A_3]'$ and $[A_4]'$. The $[Ab_i]'$ ($i = 1 - 4$) are a function of the sources of calibrator uncertainty, and can therefore be represented by the left-hand side of equation 3. Similarly, the $[A_i]'$ ($i = 1 - 4$) represent the optical absorbance values after all the sources of uncertainty operating within the calibration phase are incorporated into the model, and can therefore be represented by the left-hand side of equation 18.

These four values of RF concentrations and their corresponding optical absorbance values are used to solve for the values of the calibration parameters a', b', c' and B' . The dashed symbols for the calibration

parameters represent the incorporation of calibration uncertainty incorporated into their values. Since these form a set of nonlinear simultaneous equations, they are solved numerically using the Levenberg-Marquardt nonlinear least-squares algorithm. The calibration function with the uncertainty of the calibration phase now becomes:

$$C = \left[\frac{(a' - (A_x - B'))}{b' (A_x - B')} \right]^{1/c'} \quad (19)$$

The values of a', b', c' and B' are estimated as 42479.6, 86.1, -1.5 and 13063.7. In comparison, the corresponding parameters of the average reference function are 25100.1, 118.4, -1.6 and 12818.0.

2.2 Sample Analysis Phase

The key components of uncertainty associated with the sample analysis phase are patient sample uncertainty and instrument uncertainty. Patient sample uncertainty is generally associated with the preanalytical stage of the clinical measurement process, and is therefore out of the scope of this study. We have described the effect of instrument uncertainty in the previous section, and therefore we denote the fractional change in optical absorbance at time t due to pipetting uncertainty and clock uncertainty in the sample analysis phase as $u_{pc(m)}$. If we denote the true RF concentration in the sample as $[Ag_x]$, and the corresponding absorbance at time t as A_x , the absorbance obtained after the incorporating sample and instrument uncertainty is expressed as:

$$A'_x = A_x (1 + u_x) (1 + u_{pc(m)}) (1 + u_p) \quad (20)$$

Here A'_x represents the absorbance after the uncertainty of the sample analysis phase is introduced into the process, and u_x represents a placeholder term for the fractional change in RF concentration due to preanalytical uncertainty. The term u_p represents photometer uncertainty - we emphasize here that this term represents the random variable characterizing photometer uncertainty, and therefore its value might be different each time it is sampled in the calibration and sample analysis phase. This value of the optical absorbance is then converted into the RF concentration in the patient sample by equation 19, as shown by the expression below:

$$C'_x = \left[\frac{(a' - (A'_x - B'))}{b' (A'_x - B')} \right]^{1/c'} \quad (21)$$

The uncertainty associated with this model is estimated by generating patient sample RF concentrations (in the current implementation, 100, since it corresponds to the average number of RF tests conducted on the P-modular analytics platform in a day in a clinical laboratory) for different sets of realizations of the sources of uncertainty, and then estimating the standard deviation of these 100 recorded measurements of RF concentrations. Clock uncertainty is not included in the model implementation upon the recommendation of the manufacturer as it is negligible in practice.

Estimates of measurement uncertainty obtained from the model were compared with intermediate imprecision estimates provided by the assay manufacturer. In the absence of direct experimental validation, we elected to validate the model in such a manner because the distributional parameters of the simulation model were estimated based on the specifications provided by the assay manufacturer, which in turn were estimated from experimental data collected for each source of uncertainty. It therefore followed that model estimates of uncertainty should also be compared against the estimates of uncertainty observed experimentally by the assay manufacturer.

Estimates of uncertainty for the RF assay were provided as coefficients of variation (CVs) of 4.7% and 2.5% at RF concentrations of 17.5 IU/mL and 57.7 IU/mL, respectively. At these RF concentrations, model estimates of uncertainty were 4.14% and 2.17%, respectively - that is, the model seems to underestimate

the RF assay uncertainty. However, these comparisons are not a substitution for validation via controlled experimentation, and do not support making definitive conclusions regarding the validity of the model. In the absence of experimental validation, these comparisons provide a qualitative indication that the model provides estimates of uncertainty that are reasonable when compared to those seen in the laboratory.

3 RESULTS AND ANALYSIS

The model was programmed in the Matlab computing environment. Estimates of the rate constant k_1 (2×10^{-4} per second) and the molar absorption coefficient (14000 per IU/mL per centimeter) were based on a published experimental investigation of the kinetics of a comparable immunoassay (Nagel and Gibson 1967). In order to estimate the measurement uncertainty for patient samples whose RF concentration levels are unknown, the simulation model was used to construct an empirical function, referred to as the uncertainty profile, that generates an estimate of measurement uncertainty at a given RF concentration level. The uncertainty profile is constructed by generating uncertainty estimates at different RF concentrations in the range of possible patient sample RF concentration levels, and then finding the function that best fits the simulated data. The sample RF concentration (in IU/mL) is the independent variable, and the standard deviation (in U/L) of the distribution of the measurement result is the dependent variable. The uncertainty profile for the RF assay is shown in Figure 1, and a sample RF concentration range of 10 IU/mL - 135 IU/mL, traversed in increments of 5 IU/mL, was used in constructing the uncertainty profile.

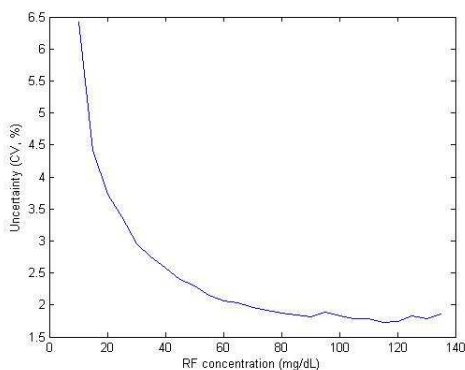


Figure 1: Uncertainty profile for the RF immunoassay.

A key use of such a model is to estimate the contributions of the sources of uncertainty operating within the measurement process. This is accomplished by setting the relevant parameters to zero (mean and standard deviation of its distribution to zero), and then re-estimating the mean and standard deviation of the measurand. The difference between the mean and the standard deviation of the measurand estimated without the source under consideration and the measurand mean and standard deviation estimated with all sources of uncertainty operating within the process represents its contribution to the inaccuracy and imprecision of the measurement process. We estimate the contributions of the sources of uncertainty operating within the sample analysis phase since these are the sources that primarily contribute to the imprecision of the measurement result, whereas the sources operating within the calibration phase contribute to the inaccuracy (bias) associated with the measurement result. The contributions of the sources of instrument uncertainty to the net assay uncertainty are summarized in Table 2.

It is clear that the reagent pipette and the sample pipette are the largest contributors to the net measurement uncertainty, and that reducing the imprecision in their operation would lead to substantial decreases in net measurement uncertainty.

We now introduce a method by which a change in uncertainty of the calibration process can be quantified without using a standard sample with an RF concentration that is established with a very high degree of

Table 2: Contribution of the sources of instrument uncertainty to net measurement uncertainty

| Source | Net uncertainty with all sources operating (CV, %) | Net uncertainty with source removed (CV, %) | % Contribution to net uncertainty |
|------------------|--|---|-----------------------------------|
| Sample pipette | 1.91 | 1.73 | 9.42 |
| Reagent pipettes | 1.91 | 0.85 | 55.50 |
| Photometer | 1.91 | 1.88 | 1.57 |

precision. We investigate the effect of increasing or decreasing uncertainty in the calibration process on the correlation structure between the parameters of the calibration function; that is, we investigate the effect of changes in calibration uncertainty on the correlation matrix of the calibration function parameters.

The parameters of the calibration function are estimated by solving a set of four nonlinear simultaneous equations that are in turn generated by four optical absorbance measurements A'_i ($i = 1-4$) recorded by analyzing four corresponding calibrators Ab'_i ($i = 1-4$). We simulate the calibration process by generating values of A'_i and the Ab'_i ($i = 1-4$) and then solving the corresponding set of nonlinear equations to generate the values of the four calibration parameters. This process is repeated 300 times and the correlation matrix between the parameters of the calibration function is generated from these simulated values of the calibration parameters.

We model the i^{th} pair of measurements (A'_i, Ab'_i) as jointly distributed random variables because each A'_i is correlated with its corresponding Ab'_i , with ρ_i being the correlation between the i^{th} pair. In order to estimate the marginal distributions of the A'_i and the Ab'_i ($i = 1-4$), the calibration process is simulated with all sources of uncertainty operating to generate 300 sets of values of A'_i and Ab'_i ($i = 1-4$). We first establish from these datasets that the A'_i and the Ab'_i are all normally distributed. The means and standard deviations of the marginal distributions of the A'_i and the Ab'_i as well as values of ρ_i are then also estimated from these simulated datasets.

Since calibrator preparation occurs prior to analysis of the calibrator on the instrument and the measurement of optical absorbance, the calibration process is simulated by first sampling from the marginal distributions of the Ab'_i , which are distributed as $N(\mu_{Ab(i)}, \sigma_{Ab(i)}^2)$ for each $i = 1-4$. Then the corresponding values of the A'_i are generated by sampling from the distributions of the A'_i , conditional on the sampled value of the Ab'_i . This is expressed in the following equation.

$$A'_i | Ab'_i \sim N\left(\mu_{A(i)} + \rho_i \frac{\sigma_{A(i)}}{\sigma_{Ab(i)}} (Ab'_i - \mu_{Ab(i)}), (1 - \rho_i^2) \sigma_{A(i)}^2\right) \quad \forall i = 1 - 4 \quad (22)$$

A change in the uncertainty of the calibration process is modeled as an increase or decrease in the standard deviations of the marginal distributions of the Ab'_i and/or the A'_i . This can be considered as an increase or decrease in the precision in the calibration process. We increased or decreased the estimates of the $\sigma_{Ab(i)}$ and the $\sigma_{A(i)}$ by factors of two and studied the effect of these changes on the correlation matrix of the parameters of the calibration function. While it was difficult to discern an easily apparent consistent change in the individual correlation coefficients between the calibration function parameters, we identified the 1-norm condition number of the correlation matrix and the sum of the absolute values of the correlation coefficients between the parameters of the calibration function as decreasing (increasing) with an increase (decrease) in calibration uncertainty. We denote the 1-norm condition number of the correlation matrix A as $\kappa_1(\mathbf{A})$, and the sum of the absolute values of the correlation coefficients between the parameters of the calibration function as $f_{\mathbf{A}}$. $f_{\mathbf{A}}$ is formally defined as follows:

$$f_{\mathbf{A}} = \frac{1}{2} \sum_{i \neq j} |\rho_{ij}| \quad (23)$$

Here ρ_{ij} represents the element in the i^{th} row and j^{th} column of \mathbf{A} . We found that an increase or decrease in $\sigma_{Ab(i)}$ does not affect the values of $\kappa_1(\mathbf{A})$ and $f_{\mathbf{A}}$; therefore, we present here the effect of simultaneously increasing or decreasing the values of the $\sigma_{A(i)}$ on $\kappa_1(\mathbf{A})$ and $f_{\mathbf{A}}$. Plots between $\kappa_1(\mathbf{A})$ and $f_{\mathbf{A}}$ versus the factors of two by which the $\sigma_{A(i)}$ are multiplied are shown in Figures 2a and 2b.

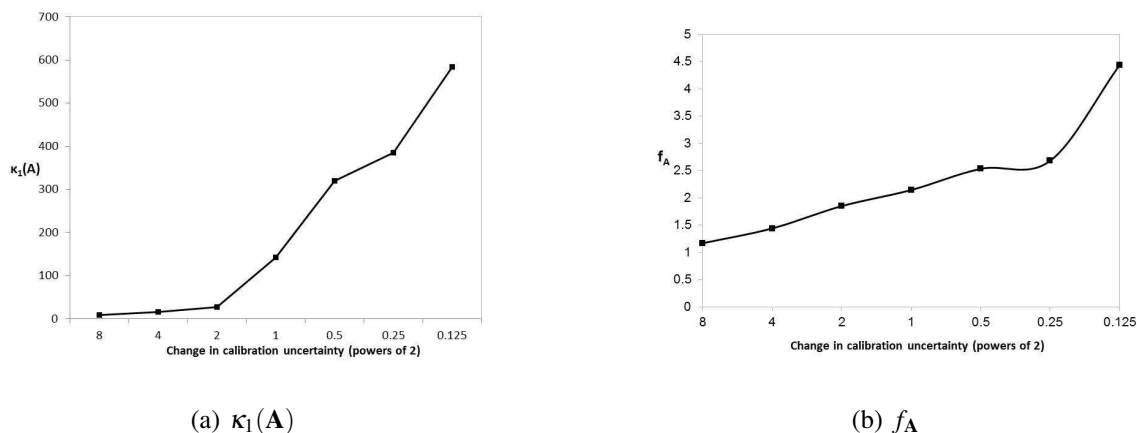


Figure 2: $\kappa_1(\mathbf{A})$ and $f_{\mathbf{A}}$ versus change in uncertainty of absorbance measurements.

We envision that the primary utility of measures such as $\kappa_1(\mathbf{A})$ and $f_{\mathbf{A}}$ is that they can be used to quantify changes in calibration uncertainty without the need for analysis of a high-precision standard sample. Their values can be estimated from calibration function parameter estimates obtained from routine calibrations. While $\kappa_1(\mathbf{A})$ exhibits greater sensitivity to change in calibration uncertainty when compared to $f_{\mathbf{A}}$, the latter is an intuitively more easily understood quantity.

4 CONCLUSIONS

The primary aim of our study is to illustrate the development of models of measurement uncertainty of immunoassays, and their use in informing laboratory practice and instrument design. We also show how the model can be used to quantify the effect of uncertainty in the sample analysis phase on the measurand distribution, and introduce $\kappa_1(\mathbf{A})$ and $f_{\mathbf{A}}$ as potential measures to quantify the change in uncertainty in the calibration phase of a measurement process. Future research will involve mathematical formalization of the use of $\kappa_1(\mathbf{A})$ and $f_{\mathbf{A}}$ to quantify change in calibration uncertainty for nonlinear measurement systems in general.

It should be mentioned here that because the purpose of this study is to describe in detail the development of an uncertainty model of an existing RF immunoassay and not to redesign the entire calibration process, we do not address the statistical considerations involved in nonlinear univariate calibration in this paper (see Forkman (2008) and Osborne (1991) for relevant discussions). Specifically, the issues associated with nonlinear inverse regression, and the choice of the inverse log-logit calibration function are beyond the scope of this paper. Further, while the identification of optimal calibrator concentrations that minimize net assay uncertainty has been explored previously in the context of linearly calibrated assays (Ramamohan et al. 2014), we do not address this issue in this study because the primary aim of this paper is to describe the development of an uncertainty model for an immunoassay with predetermined calibrator concentrations. We plan to address this issue in a future study, building upon previous work by Forkman (2008).

REFERENCES

- Aronsson, T., C.-H. de Verdier, and T. Groth. 1974. "Factors Influencing the Quality of Analytical Methods: A Systems Analysis, with Use of Computer Simulation". *Clinical Chemistry* 20 (7): 738–748.
- BIPM, IEC, IFCC, ISO, IUPAC, IUPAP, and OIML. 1993. *Guide to the Expression of Uncertainty in Measurement*. Geneva: ISO.
- Borg, L., J. Kristiansen, J. M. Christensen, K. F. Jepsen, and L. K. Poulsen. 2002. "Evaluation of Accuracy and Uncertainty of ELISA Assays for the Determination of Interleukin-4, Interleukin-5, Interferon- γ and Tumor Necrosis Factor- α ". *Clinical Chemistry and Laboratory Medicine* 40 (5): 509–519.
- Burtis, C. A., E. R. Ashwood, and D. E. Bruns. 2012. *Tietz Textbook of Clinical Chemistry and Molecular Diagnostics*. Elsevier Health Sciences.
- Ferri, F. 2012. *Ferri's Clinical Advisor 2013: 5 Books in 1*. Mosby Elsevier.
- Forkman, J. 2008. "A Method for Designing Nonlinear Univariate Calibration". *Technometrics* 50 (4): 479–486.
- JCGM-100 2008. "Evaluation of Measurement Data – Guide to the Expression of Uncertainty in Measurement". Technical report, BIPM.
- JCGM-101 2008. "Evaluation of Measurement Data – Supplement 1 to the "Guide to the Expression of Uncertainty in Measurement" – Propagation of Distributions Using a Monte Carlo method". Technical report, BIPM.
- Kallner, A. 1999. "Quality Specifications Based on the Uncertainty of Measurement". *Scandinavian Journal of Clinical and Laboratory Investigation* 59 (7): 513–516.
- Kragten, J. 1994. "Calculating Standard Deviations and Confidence Intervals with a Universally Applicable Spreadsheet Technique". *Analyst* 119:2161–2165.
- Kristiansen, J. 2001. "Description of a Generally Applicable Model for the Evaluation of Uncertainty of Measurement in Clinical Chemistry". *Clinical Chemistry and Laboratory Medicine* 39 (10): 920–931.
- Krouwer, J. 2002. "Setting Performance and Evaluating Total Analytical Error for Diagnostic Assays". *Clinical Chemistry and Laboratory Medicine* 48 (6): 919–927.
- Nagel, R. L., and Q. H. Gibson. 1967. "Kinetics and Mechanism of Complex Formation Between Hemoglobin and Haptoglobin". *Journal of Biological Chemistry* 242 (15): 3428–3434.
- Osborne, C. 1991. "Statistical Calibration: A Review". *International Statistical Review*:309–336.
- Ramamohan, V., J. T. Abbott, G. Klee, and Y. Yih. 2014. "Modeling, Analysis and Optimization of Calibration Uncertainty in Clinical Laboratories". *Measurement* 50:175–185.
- Rami, L., and F. Canalias. 2014. "An Approach to Establish the Uncertainty Budget of Catalytic Activity Concentration Measurements in a Reference Laboratory". *Clinical Chemistry and Laboratory Medicine*.
- Suchanek, M., and P. Robouch. 2009. "Measurement Uncertainty of Test Kit Results – the ELISA Example". *Clinical Chemistry and Laboratory Medicine* 47 (7): 808–810.

AUTHOR BIOGRAPHIES

VARUN RAMAMOHAN is a Senior Research Health Economist working with the Research Triangle Institute (Health Solutions). He holds a Ph.D. in Industrial Engineering from Purdue University. His email address is varun.ramamohan@gmail.com.

JAMES T. ABBOTT heads the Clinical Support Group at the Roche Diagnostics Corporation. He holds a Ph.D. in Chemistry from Queen's University in Northern Ireland. His email address is jim.abbott@roche.com.

YUEHWERN YIH is a Professor in the School of Industrial Engineering at Purdue University. She holds a Ph.D. in Industrial & Systems Engineering from the University of Wisconsin, Madison. Her email address is yih@purdue.edu.